A Micro-Scale Approach for Cropland Suitability Assessment of Permanent Crops Using Machine Learning and a Low-Cost UAV

Article *in* Agronomy · January 2023

DOI: 10.3390/agronomy13020362

5 authors, including:

Dorijan Radocaj
University of Osijek
36 PUBLICATIONS **311** CITATIONS
SEE PROFILE

Ante Šiljeg
University of Zadar
90 PUBLICATIONS **307** CITATIONS
SEE PROFILE

Ivan Plaščak
University of Osijek
51 PUBLICATIONS **174** CITATIONS
SEE PROFILE

Ivan Marić
University of Zadar
64 PUBLICATIONS **200** CITATIONS
SEE PROFILE

agronomy

MDPI

Article

A Micro-Scale Approach for Cropland Suitability Assessment of Permanent Crops Using Machine Learning and a Low-Cost UAV

Dorijan Radočaj [1,*], Ante Šiljeg [2], Ivan Plaščak [1], Ivan Marić [2] and Mladen Jurišić [1]

[1] Faculty of Agrobiotechnical Sciences Osijek, Josip Juraj Strossmayer University of Osijek, Vladimira Preloga 1, 31000 Osijek, Croatia
[2] Department of Geography, University of Zadar, Franje Tuđmana 24 i, 23000 Zadar, Croatia
* Correspondence: dradocaj@fazos.hr; Tel.: +385-31-554-965

Abstract: This study presents a micro-scale approach for the cropland suitability assessment of permanent crops based on a low-cost unmanned aerial vehicle (UAV) equipped with a commercially available RGB sensor. The study area was divided into two subsets, with subsets A and B containing tangerine plantations planted during years 2000 and 2008, respectively. The fieldwork was performed on 27 September 2021 by using a Mavic 2 Pro UAV equipped with a commercial RGB sensor. The cropland suitability was performed in a two-step classification process, utilizing: (1) supervised classification with machine learning algorithms for creating a vegetation mask; and (2) unsupervised classification for the suitability assessment according to the Food and Agriculture Organization of the United Nations (FAO) land suitability standard. The overall accuracy and kappa coefficients were used for the accuracy assessment. The most accurate combination of the input data and parameters was the classification using ANN with all nine input rasters, managing to utilize complimentary information regarding the study area spectral and topographic properties. The resulting suitability levels indicated positive suitability in both study subsets, with 63.1% suitable area in subset A and 59.0% in subset B. Despite that, the efficiency of agricultural production can be improved by managing crop and soil properties in the currently non-suitable class (N1), providing recommendations for farmers for further agronomic inspection. Alongside low-cost UAV, the open-source GIS software and globally accepted FAO standard are expected to further improve the availability of its application for permanent crop plantation management.

Keywords: unmanned aerial vehicle; tangerine plantation; vegetation index; FAO land suitability; artificial neural network; open-source GIS software

Citation: Radočaj, D.; Šiljeg, A.; Plaščak, I.; Marić, I.; Jurišić, M. A Micro-Scale Approach for Cropland Suitability Assessment of Permanent Crops Using Machine Learning and a Low-Cost UAV. *Agronomy* **2023**, *13*, 362. https://doi.org/10.3390/agronomy13020362

Academic Editors: Jitka Kumhálová, Jan Lukáš, Pavel Hamouz and Jose Antonio Dominguez-Gómez

Received: 29 November 2022
Revised: 23 January 2023
Accepted: 25 January 2023
Published: 26 January 2023

1. Introduction

For economies to sustain, permanent natural resources including climate, soil, and topography should be used rationally and sustainably for agricultural production [1]. The World Commission on Environment and Development defines sustainable development as meeting current agricultural production demands without compromising the capacity of future generations to meet their own needs [2]. In addition, more crop yield is needed to provide necessities because of fast population expansion and migration [3]. Natural resources including forests, pastures, wetlands, and agricultural fields are converted into settlements or industrial zones, which results in the underutilization of these regions [4]. Therefore, it is crucial to develop a land management plan which supports the conservation and optimal usage of natural resources for future generations. Determining whether a particular land is suitable for agriculture is a necessary step in land use planning [5]. A decision to employ existing natural resources based on the predicted cropland suitability is made as part of the process of determining amenities [6]. The process of assessing a

specific area of land suitability, such as in agriculture or forestry, and its level of environmental sustainability, is known as cropland suitability assessment [7]. The analysis of complementary abiotic environmental data, climate, soil, and topography, is required to determine the suitability of agricultural land [8]. As permanent crops require initial substantial investments and the long-term commitment of the agricultural land, suitability analyses are particularly of interest for agricultural land management [9]. This approach also enables the rational utilization of the abandoned agricultural land for the cultivation of permanent crops, positively affecting the sustainability of agricultural production [10].

Open data remote sensing satellite missions can observe the surface of the Earth with a spatial resolution in the range between 10 m and 1 km [11]. Due to the relationship of reflectance in the visible, red-edge, and near-infrared spectral bands with crop health and growth, they are frequently employed to evaluate cropland suitability [12]. Missions with moderate spatial resolution, such as Landsat and Sentinel-2 missions, are frequently employed in agriculture, and their temporal resolution spans from a few days to two weeks [13]. The fact that most of the world's land is frequently obscured by clouds, impairing the Earth observation from space, is one of the main obstacles to utilizing satellites to monitor the Earth's surface for agricultural purposes [14]. Their spatial resolution is too low to detect vegetation properties on a sub-decimeter level in smaller agricultural parcels typical for permanent crops, which is another problem [15]. This is crucial because only spatial patterns or textures that are discernible at reasonably high spatial resolution may be used to identify changes in vegetation growth [16]. As a result, satellite missions cannot fully address the remote sensing needs of agriculture. Therefore, unmanned aerial vehicles (UAVs) became highly popular to close the gaps in observing such agricultural fields [17]. The RGB (red-green-blue) and multispectral sensors mounted on UAVs can be tuned to monitor crop health, allowing farmers to react in time and apply the necessary fertilizer and insecticide [18]. UAVs are used to monitor the field in 3D for early soil analysis that is required for the planning of seeding using the variable-rate-technology (VRT) principles in precision agriculture [19]. After sowing, these data are used to plan irrigation, and for the required amounts of nitrogen in certain zones of the cultivated area [20]. UAVs are also used for crop spraying, using sensors to apply the needed pesticide amount in a specific location [21]. As a result, a reduced quantity of fertilizers and pesticides are applied, reducing groundwater contamination. The application of aerial spraying using UAVs might even reduce the spraying duration multiple times compared to traditional spraying [22].

Vegetation indices are frequently utilized to quantify crop properties, out of which the most commonly used is the normalized difference vegetation index (NDVI) [23]. However, its computation requires farmers to acquire multispectral sensors mounted on UAVs, which might not be affordable in less developed parts of the world. To overcome this, researchers focused on the development of processing methods that utilize UAV images obtained by low-cost RGB sensors. Various spectral indices, as alternatives to NDVI which utilize blue, green, or red spectral bands, were developed and evaluated in the process. These include the normalized green-red difference index (NGRDI) [24], green leaf index (GLI) [25], and Kawashima index (IKAW) [26]. Such studies successfully implemented these indices collected using low-cost UAVs in crop monitoring [27], creating prescription maps in precision agriculture [28], and analyzing specific phenological stages [29]. Meanwhile, no comprehensive methodology for cropland suitability assessment utilizing low-cost UAVs was developed so far at a micro-scale, being largely focused on the macro-scale areas, such as national or county scales [30,31]. Besides data collection using low-cost UAVs, the image processing segment using the open-source geographic information system (GIS) software complements the global accessibility to farmers by ensuring state-of-the-art machine learning classification methods [32].

The aim of this study was to provide a framework for the cropland suitability assessment by combining two requirements for effective agricultural land management at a micro-scale: (1) using a low-cost UAV equipped with the commercially available RGB sensor,

and (2) using open-source GIS software for the cropland suitability assessment. These components provide a widespread solution to the farmers by minimizing their initial financial expenditures in planning the utilization of agricultural land. This study specifically focused on the cropland suitability of permanent crops, using tangerine plantation as a reference case.

2. Materials and Methods

2.1. Study Area

The study area is located in southern Croatia, in the Neretva river valley (17°32′ E, 43°01′ N) (Figure 1). The specificity of agricultural production in this area is the proximity to the sea, a warmer climate which during the summer extends into the fall, and the colder weather lasts longer during the spring [33]. The average amount of precipitation in the study area is about 1300 mm per year, but farmers face a problem when 65–75% of that amount falls during the winter. Therefore, the irrigation system network that has been created is extremely relied upon for agricultural production. The study area was divided into two subsets, with subsets A and B containing tangerine plantation planted during years 2000 and 2008, respectively. The total study area covers 1.94 ha, with each subset covering the equal area of 0.97 ha.

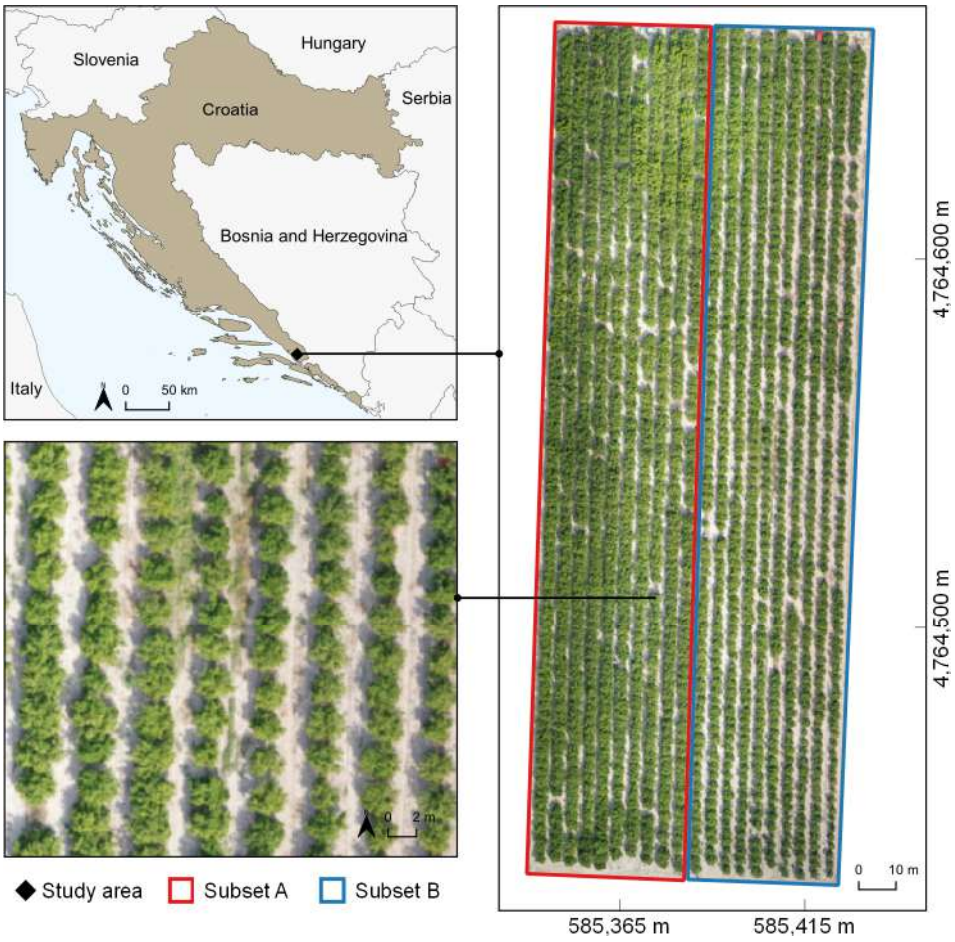

Figure 1. Tangerine plantation subsets in the Neretva river valley representing a study area.

2.2. Fieldwork and Data Acquiring

The fieldwork was performed on 27 September 2021, starting at 10 a.m. local time by study area reconnaissance and setting up global navigation satellite system (GNSS) orientation points for the georeferencing of UAV imagery. A total of 10 GNSS orientation points were placed regularly over a study area, and their coordinates were acquired using a

Trimble R8x GNSS receiver with the Croatian Positioning System (CROPOS). Its high-precision positioning service enabled real-time-kinematic (RTK) positioning with 2 cm horizontal and 4 cm vertical accuracy [34]. The fieldwork preceded a beginning harvest of tangerines, which began to mature in the study area, as displayed in Figure 2.

Figure 2. A terrestrial representation of tangerine trees during the fieldwork in the study area.

A low-cost Mavic 2 Pro UAV equipped with a 1″ CMOS RGB sensor [35] was used for image collection. The images were acquired from a relative flight altitude of 50 m, resulting in a total of 137 images over a 2.0 ha area. Image overlap was set to 80% for front and 70% for side overlap. The photogrammetry processing was performed in Agisoft Metashape Professional software v1.5.2 (St. Petersburg, Russia) using the Structure-from-motion algorithms. The dense point cloud consisted of 5,316,064 points, producing the spatial resolution of the digital orthophoto and digital surface model of 1.1 cm and 8.9 cm, respectively. Both rasters were reprojected to the Croatian Terrestrial Reference System (HTRS96/TM, EPSG: 3765) and harmonized to the 10 cm spatial resolution.

2.3. Input Data for Cropland Suitability Assessment

Data processing in GIS was performed in two open-source software, SAGA GIS v7.9.0 (Göttingen, Germany) and QGIS v3.10 (Grüt, Switzerland). The input data consisted of three primary data groups: (1) spectral bands, (2) spectral indices, and (3) topographic indices. The spectral bands consisted of blue (B), green (G) and red (R) spectral bands expressed in 8-bit digital number (DN) values ranging from 0 to 255. These were used for the calculation of three spectral indices: NGRDI, GLI and IKAW, which enabled the characterization of vegetation properties in previous studies [24,25,28]. Moreover, these indices focus either on quantifying vegetation variability using green and red reflectance (NGRDI), using red and blue reflectance as a complementary index to NGRDI (IKAW) [36], or utilizing the combination of all three visible bands for the representation of biomass [37]. These indices represented an alternative to more popular indices, such as NDVI, which could be utilized with the low-cost UAVs equipped with RGB sensor [38]. Despite utilizing only spectral information from the visible part of the spectrum, NRGDI and GLI reliably represent vegetation leaf area index, producing a high correlation in a study by Liu and Wang [39]. The selected spectral indices were calculated according to the equations displayed in Table 1.

Table 1. Spectral indices used in the study.

Spectral Index	Abbreviation	Equation	Reference
Normalized Green Red Difference Index	NGRDI	$NGRDI = \frac{G - R}{G + R}$	[40]
Green Leaf Index	GLI	$GLI = \frac{2G - R - B}{2G + R + B}$	[41]
Kawashima index	IKAW	$IKAW = \frac{R - B}{R + B}$	[42]

In contrast to the spectral data defined in the two-dimensional area by spectral bands and indices, the third input data group completed the three-dimensional representation of the study area by including three topographic indices derived from the digital surface model. These were potential annual total insolation [43], flow accumulation [44] and wind exposition [43] calculated in SAGA GIS v7.9.0 (Göttingen, Germany). The potential total insolation was calculated as a sum of direct and diffuse insolation during the year 2022, using a solar constant of 1367 Wm^{-2}, and generalizing atmospheric effects by a 70% lumped atmospheric transmittance parameter. Flow accumulation modelled the intensity of surface water retention in the field expressed in down flow area, using the multiple flow direction method proposed by Freeman [45]. Wind exposition was represented as a dimensionless index, with its values proportionally indicating areas more sheltered (below 1) and exposed (above 1) to wind. Correlation analysis using Pearson's correlation coefficient of all nine input rasters was performed to evaluate the complementarity of input data [46]. The individual rasters from three input data groups used in the study are presented in Figure 3.

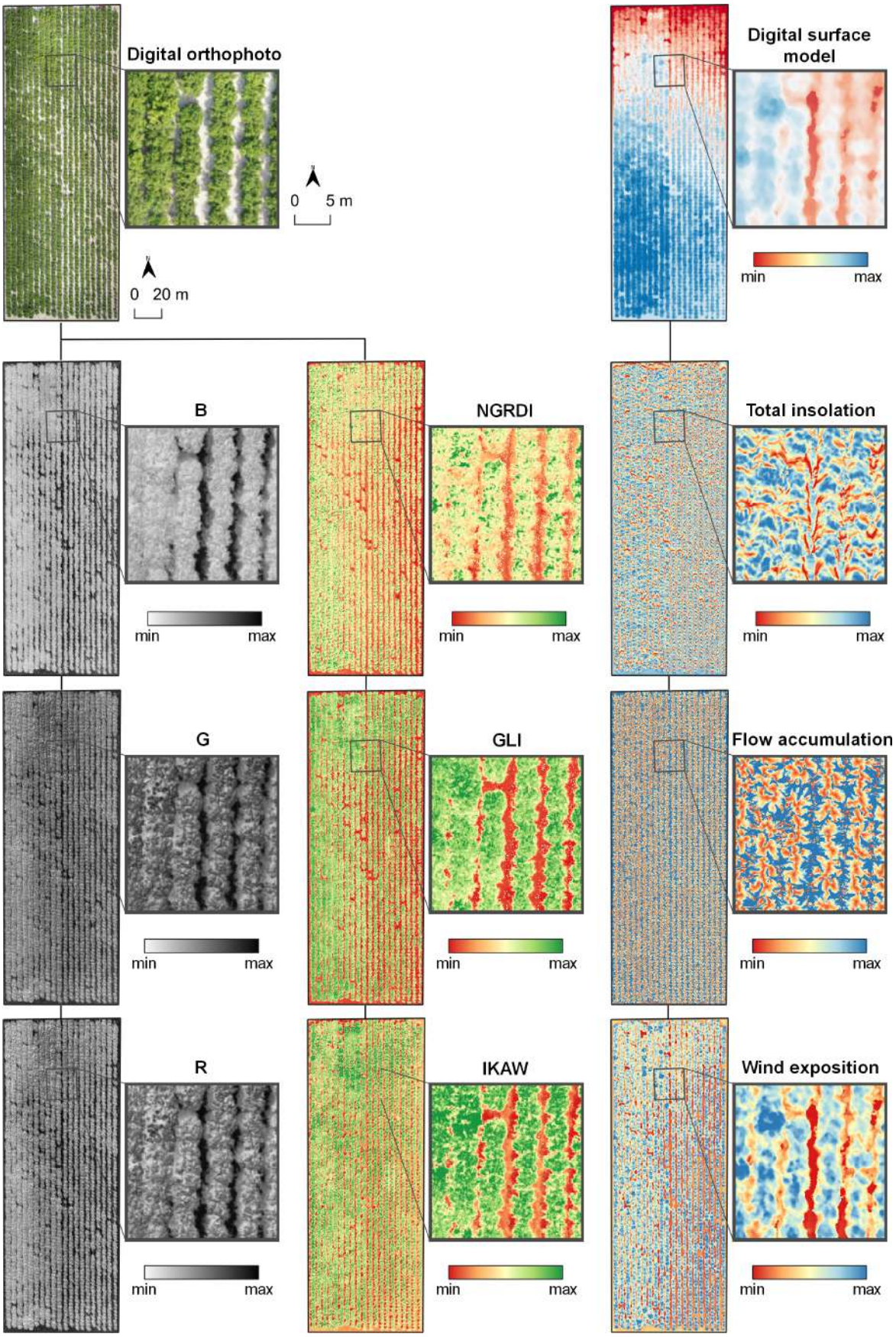

Figure 3. The display of input data used for the cropland suitability assessment from the digital orthophoto and digital surface model using low-cost UAV imaging.

2.4. Cropland Suitability Assessment

The proposed cropland suitability assessment method for permanent crops at the micro-scale based on low-cost UAV imaging is summarized in Figure 4. The fundamental suitability assessment approach relies on two-step classification: (1) supervised classification using machine learning to reliably determine vegetation mask and remove non-vegetation areas from further processing; and (2) unsupervised classification using K-means to rank vegetation classes according to Food and Agriculture Organization of the United Nations (FAO) standard for land suitability assessment [47].

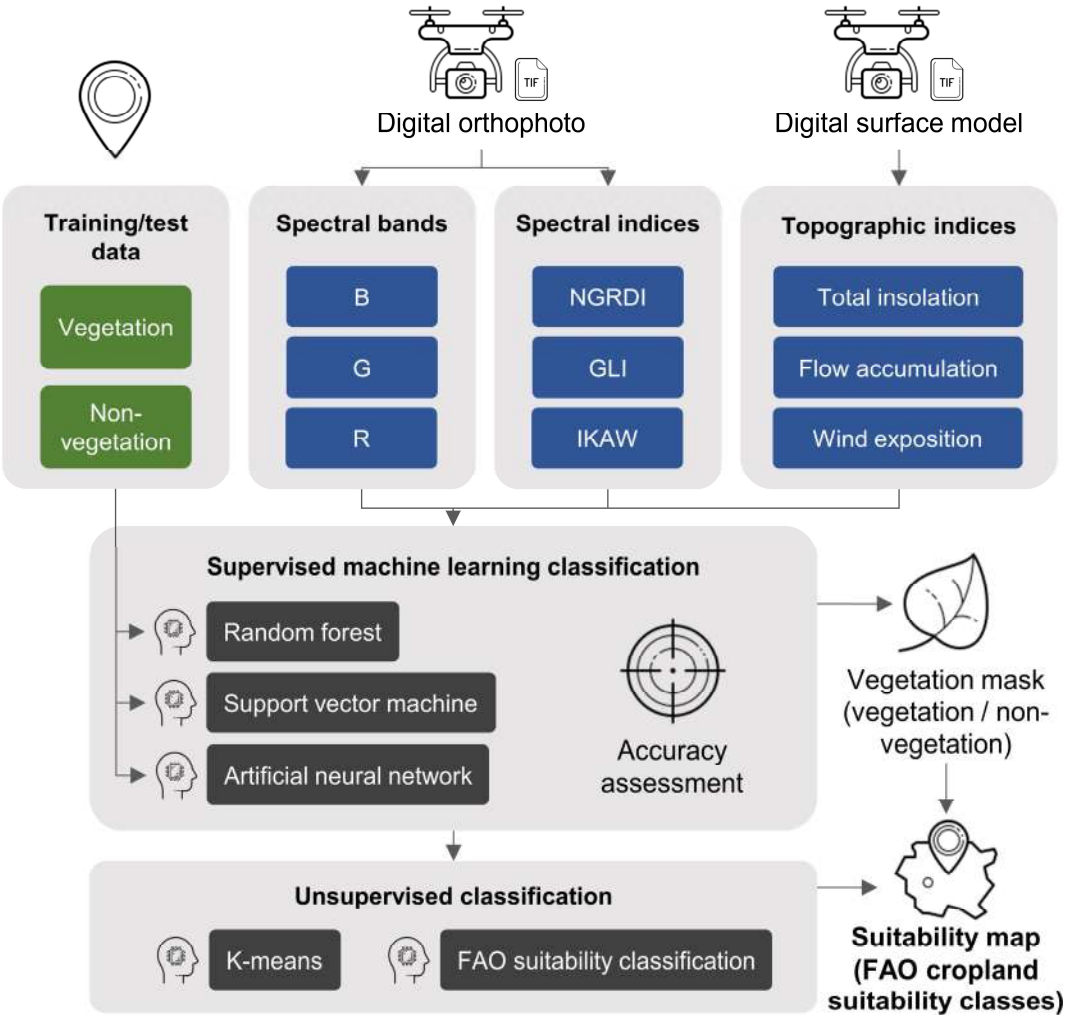

Figure 4. The proposed cropland suitability assessment method at the micro-scale.

Training/test data were delineated according to the ground truth observations into two classes (vegetation and non-vegetation). The total area of training/test data was 368.5 m², covering 1.9% of the study area. The division of training and test data was performed using the stratified random split to a 60/40 ratio, creating training and test data sets covering the area of 221.1 m² (1.1% of the study area) and 147.4 m² (0.8% of the study area), respectively. The input data into supervised classification using machine learning was evaluated in three variants: variant 1 with three rasters (spectral bands), variant 2 with six rasters (spectral bands and indices), and variant 3 with nine rasters (spectral bands and indices, topographic indices). Three machine learning algorithms were evaluated as well according to recommendations in previous research [48], including Random Forest (RF), Support Vector Machine (SVM), and Artificial Neural Network (ANN). Besides their robustness and high classification accuracy, the selection of these three methods comprises

representative methods of established machine learning approaches: RF for ensemble decision trees, ANN for artificial neural networks and SVM for supervised support vector machines [49]. The parameters for supervised classification were evaluated and selected on an iterative basis, according to the highest reached overall accuracy. RF was performed with the maximum tree depth of 25 and 1SE (one-standard-error) rule to ensure a higher resistance to training data noise and to produce more compact decision trees. The selected SVM type for the classification was c-support vector classification with a polynomial kernel and a gamma coefficient of 1. ANN consisted of five layers in the network, not including input and output layers, each with five neurons. The maximum number of iterations was set to 300 and activation was performed using the sigmoid function. The accuracy assessment of the supervised classification was performed using the error matrix, as a standard descriptive tool for evaluating the classification accuracy of remotely sensed data [50]. Overall accuracy and kappa coefficients quantified the accuracy, with higher values proportionally indicating higher classification accuracy.

According to the most accurate supervised classification result, non-vegetation pixels were dissolved and extracted from the study area, providing a vegetation mask for the unsupervised classification. The nine input rasters were clipped to the extent of the vegetation mask and inputted in the K-means unsupervised classification using the Hill-Climbing variant in five classes. The resulting classes were ranked according to the FAO land suitability specifications [51], designating the highly suitable (S1), moderately suitable (S2), marginally suitable (S3), currently non-suitable (N1), and permanently non-suitable (N2) classes.

3. Results

The correlation matrix justifies the selection of three input data groups (spectral bands, spectral indices, topographic indices), as individual rasters from their respective groups resulted in low correlation with rasters from other groups. As for the within-group relationships, R with G and B resulted in an extreme Pearson's correlation coefficient (Figure 5).

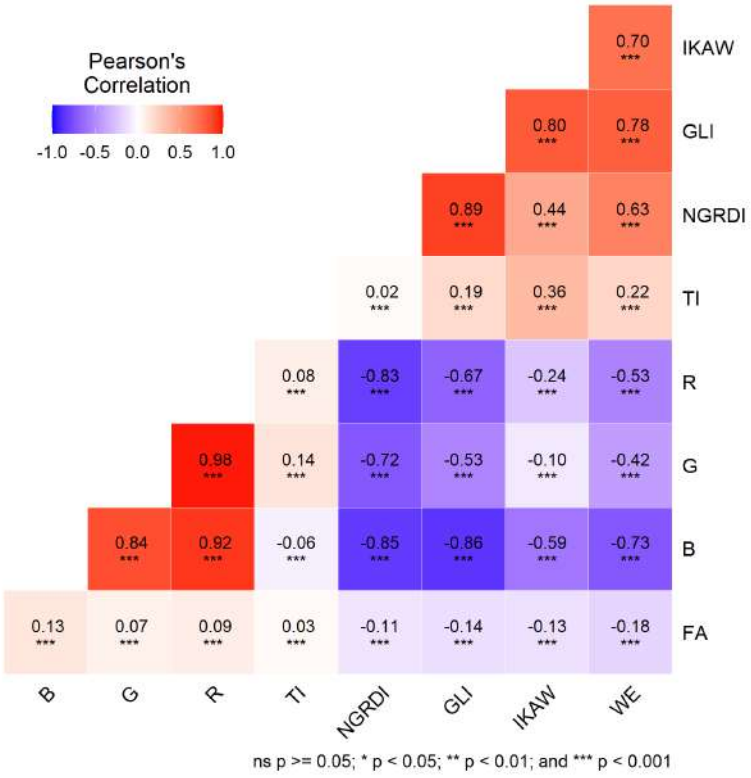

Figure 5. Correlation matrix based on Pearson's correlation coefficients (TI: total insolation, FA: flow accumulation, WE: wind exposition).

All three evaluated machine learning algorithms for the supervised classification of vegetation and non-vegetation areas enabled high reliability in creating vegetation mask (Table 2). The most accurate combination of the input data and parameters was the classification using ANN with all nine input rasters, managing to utilize complimentary information regarding study area spectral and topographic properties. This combination resulted in the highest overall accuracy and kappa coefficient, performing especially well in recognizing non-vegetation areas (Figure 6). The RF classification results also enabled very high accuracy in creating vegetation mask, ranking a close second behind ANN. Meanwhile, SVM was very sensitive to the selection of input rasters, resulting in the lowest classification accuracy for all variants. Figure 7 displays the distribution of training/test data for supervised classification in the study area, as well as the resulting vegetation mask from the most accurate classification result.

Table 2. Accuracy assessment of the supervised classification results for the creation of vegetation mask.

Classification Algorithm	Input Data	Overall Accuracy	Kappa
RF	Variant 1	0.994	0.984
	Variant 2	0.993	0.981
	Variant 3	0.994	0.985
SVM	Variant 1	0.907	0.762
	Variant 2	0.964	0.903
	Variant 3	0.965	0.911
ANN	Variant 1	0.993	0.983
	Variant 2	0.995	0.988
	Variant 3	0.996	0.990

Variant 1: spectral bands; Variant 2: spectral bands and indices; Variant 3: spectral bands and indices, topographic indices.

		Random Forest			Support Vector Machine			Artificial Neural Network		
		Non-vegetation	Vegetation	Commission error	Non-vegetation	Vegetation	Commission error	Non-vegetation	Vegetation	Commission error
Variant 1	Non-vegetation	4231	37	0.009	3491	675	0.162	4218	24	0.006
	Vegetation	64	11,513	0.006	804	10,875	0.069	77	11,526	0.007
	Omission error	0.015	0.003		0.187	0.058		0.018	0.002	
Variant 2	Non-vegetation	4245	45	0.011	3865	164	0.047	4305	52	0.012
	Vegetation	64	11,491	0.006	390	11,408	0.034	21	11,467	0.002
	Omission error	0.015	0.004		0.101	0.016		0.005	0.005	
Variant 3	Non-vegetation	4239	20	0.005	3883	164	0.042	4284	23	0.005
	Vegetation	70	11,516	0.006	391	11,407	0.034	40	11,498	0.003
	Omission error	0.017	0.002		0.101	0.014		0.009	0.002	

Figure 6. Error matrices from three evaluated machine learning algorithms and three input data variants.

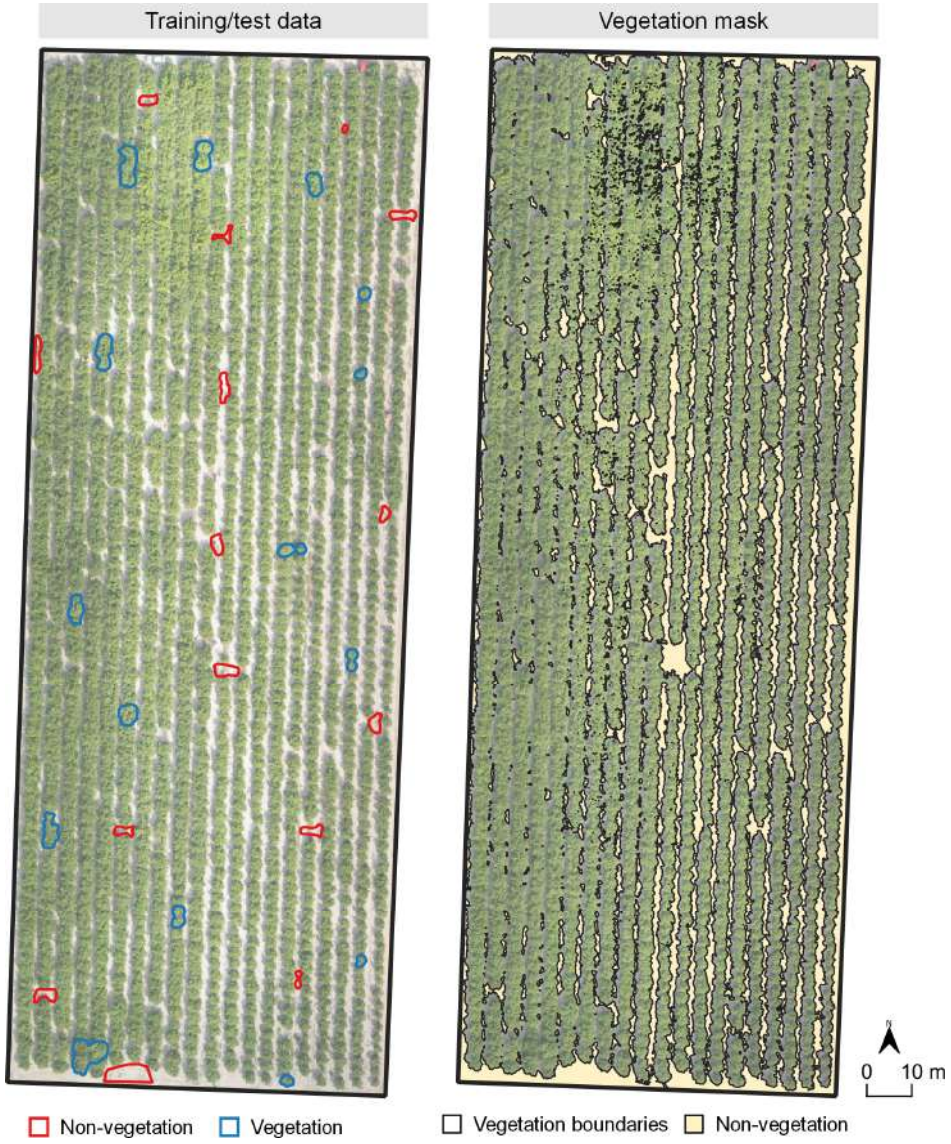

Figure 7. The display of training/test data used for supervised classification and the vegetation mask calculated from the classification.

The results from the unsupervised classification, ranked according to the FAO suitability standard, showed a similar representation of individual suitability classes in both study subsets regarding the relative area, while subset A covered a larger area due to higher biomass (Table 3). The total area of suitable classes in subsets A and B resulted in 63.1% and 59.0%, respectively, while the lowest class area indicated permanently non-suitable land for tangerine cultivation. Class means results showed variability, particularly for topographic indices, total insolation, and flow accumulation (Table A1). The final suitability map produced by the proposed cropland suitability assessment method at the micro-scale is presented in Figure 8.

Table 3. The absolute and relative area of FAO suitability classes for tangerine cultivation.

Study Area Subset	Area per FAO Suitability Class				
	S1	**S2**	**S3**	**N1**	**N2**
Subset A	2493.7 m² (28.5%)	2060.8 m² (23.1%)	1020.8 m² (11.5%)	2698.5 m² (30.7%)	536.4 m² (6.2%)
Subset B	1787.0 m² (24.3%)	1621.3 m² (22.0%)	922.5 m² (12.7%)	2383.3 m² (32.6%)	645.7 m² (8.4%)

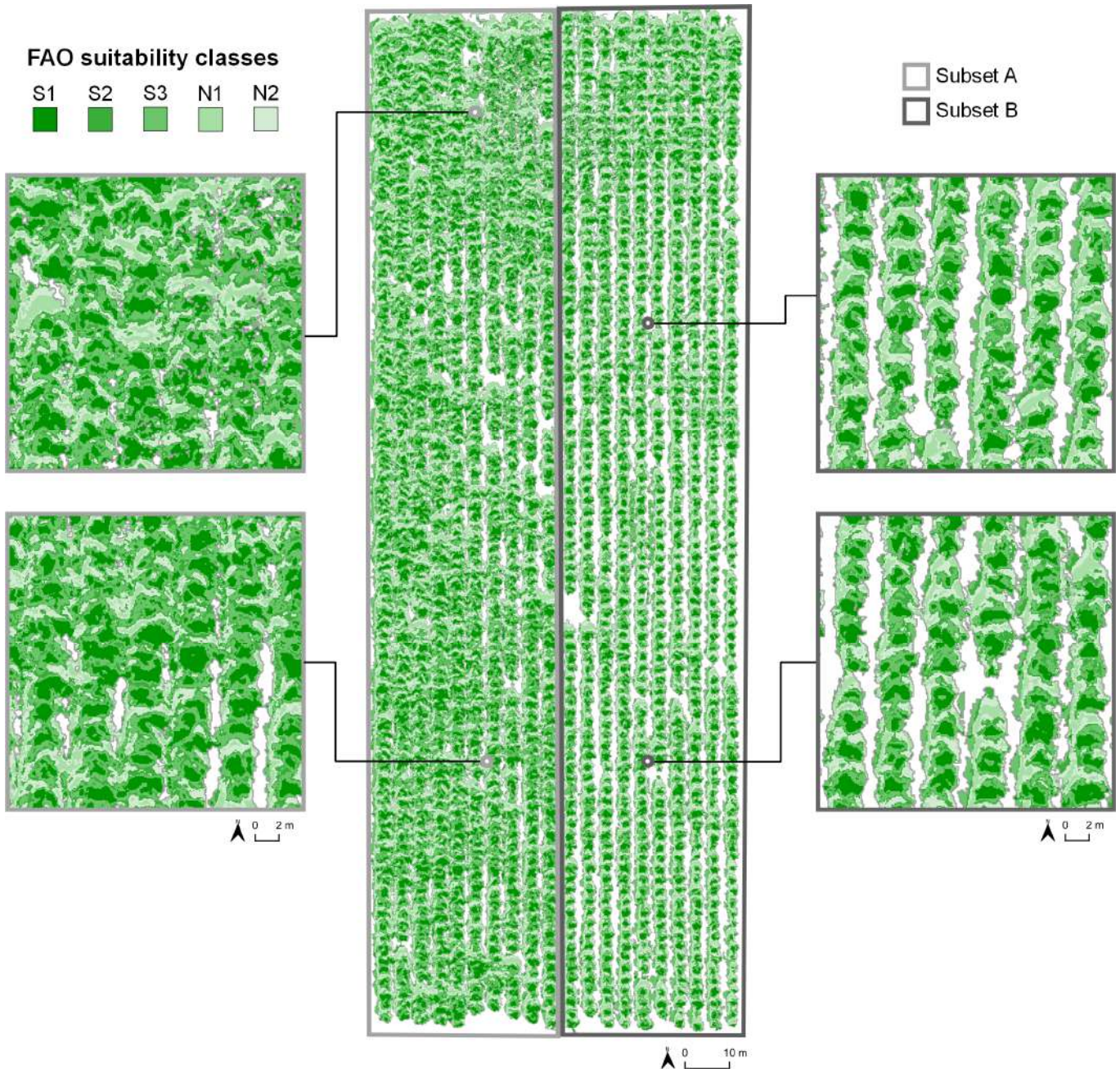

Figure 8. The final suitability map produced by the proposed cropland suitability assessment method at the micro-scale.

4. Discussion

The application of UAVs in agriculture is becoming common, as is the use of other machinery for agricultural production. The major impact is the low cost of UAVs compared to state-of-the-art agricultural machinery [19], and it allows for advanced crop monitoring that gives the farmer a lot of information to work with. By adjusting land management plans according to cropland suitability assessment results, farmers can increase yields and reduce crop damage [8]. The amount of mineral fertilizer and pesticides is also reduced, which has a positive effect on the environment [52]. While a low-cost UAV equipped with an RGB sensor presents an affordable solution for cropland suitability assessment and crop monitoring at a micro-scale, they provide restricted observation capabilities in agriculture. UAVs with hyperspectral, multispectral, or thermal sensors, can more reliably detect water stress in crops to determine which parts of the agricultural area

need irrigation [53]. Furthermore, it is possible to calculate significantly more vegetation indices, which determine the relative density and health of the crop [54]. Measurements spanning several narrow-band waves (10 nm) with additional bands in the visible, near-infrared, and the short-wave infrared regions of the spectrum are also made possible via hyperspectral sensors [55]. Thus, more accurate vegetation indices are produced by choosing significant bands in hyperspectral data, which is essential for enhancing the efficiency of LAI index calculation [56]. Novel technologies such as high throughput phenomics can additionally enhance crop health assessment, providing a better insight into abiotic stress tolerance using automated solutions based on remote sensing [57]. Nevertheless, low-cost UAVs equipped with RGB cameras are presently available for a wide range of farmers looking to make initial cropland suitability analyses based on vegetation indices and topographic properties as used in this study.

To maximize the accuracy of suitability assessment results, this study reinforced the necessity to evaluate several input data variants and machine learning classification algorithms. Several previous studies confirmed these findings, especially considering vegetation indices calculated from the data from the visible part of the spectrum, obtainable by low-cost RGB sensors. Early research by Hunt et al. [58] examined the relationship between alfalfa, maize, and soybean biomass levels, and the NGRDI index. Higher mean visible reflectance for a particular NGRDI showed that low chlorophyll content was related to greater intensity. To further increase its applicability in cropland suitability studies, the red spectrum of the digital camera's red filter might be moved to a longer wavelength (about 680 nm), which would make NGRDI more sensitive to variations in chlorophyll content [59]. In the study by García-Martínez et al. [60], the triangular greenness index (TGI) and object-oriented classification were used to analyze the green cover, and a correlation coefficient of 0.77 was found between the green cover and maize grain yield. Additionally, the findings from the study of Hunt et al. [61] showed that TGI has the potential for managing nitrogen fertilizer until was saturated at high amounts of chlorophyll concentration but the correlation was independent of the spectral resolution of the sensor. These findings could provide a basis for the upgrade of the proposed cropland suitability assessment methods at the micro-level for the variable rate application in precision agriculture, providing the required crop potential zones [62]. The creation of input data variants with three increasingly complex levels of image preprocessing collected using UAV with RGB camera, with variant based on spectral bands as a baseline, indicated a constant minor classification superiority of all evaluated input data. While using the most affordable UAVs in crop suitability assessment, this study supported the previous observation of the advantage of time investment in image preprocessing, resulting in a cost-efficient increase in classification accuracy [63]. Despite RF frequently being more accurate to SVM and ANN based on UAV images for cropland suitability and health analyses [64,65], there is an increasing number of cases in which ANN provides superior results in permanent and perennial crop analyses in comparison to RF, SVM, and similar machine learning methods. Besides its superiority in tangerine plantation suitability assessment from this study, Syazwani et al. [66] achieved the highest accuracy using ANN in precision agriculture of pineapple plantation, while Khan et al. [67] noted its popularity in various segment of oil palm cultivation. Nevertheless, due to classification accuracy results being dependent on input data properties, it is still important to evaluate multiple machine learning methods to ensure optimal solution for a particular case [68].

Along with the analysis of vegetation indices, it is advisable to regularly perform soil analysis in order to increase yields and reduce production costs as part of cropland suitability analysis. Present regulations for soil analysis in Croatia [69] require only one sample per parcels with an area larger than 1 ha, collected as the average from 20–25 subsamples. Therefore, conventional soil sampling regulations disregard in-field variabilities and provide an overview of generalized soil condition. With the proposed cropland suitability assessment approach, farmers can identify low performance areas and collect additional samples in critical areas and using this information to detect nutrient deficiency in such

areas. The tangerine plantations in the study area are very sensitive to soil sodium content, whose high amount impairs yield quality [70]. Regular water analysis for irrigating and monitoring the level of sodium in the soil are required to lessen the detrimental effects of sodium. These insights, along with the vegetation mask creation approach for the differentiation of vegetation and non-vegetation areas prior to cropland suitability classification, strongly indicate that the proposed approach can be viable for a number of similar permanent crops. By applying microelements through foliar fertilization, permanent crops can receive sufficient amounts of elements necessary for growth and development regardless of poor soil conditions [71].

Future uses of remote sensing in agronomic management will frequently expand on the principles of conventional methods. Combining several vegetative indicators to calculate agricultural productivity is one of the remote sensing technologies' unrealized potentials [72]. To represent spatio-temporal patterns in crops and soils, the data from vegetation indices could be enriched with climate data in order to provide useful information for decision-making [73]. Claverie et al. [74] used this approach for maize and sunflower, combining biomass phenology data throughout their vegetative season. Using a crop suitability model and remote sensing, they linked the phenology stages of plant development yield prediction. Different wavelengths were identified by Guan et al. [75] to be able to predict agricultural production, although climate data was necessary for the assessment of crop growth characteristics. In widening the scope of cropland suitability using the biophysical properties, Zarco-Tejada et al. [76] investigated the application of chlorophyll fluorescence for the estimation of net photosynthesis. As crop growth enables most of the background soil visible until the crop entirely covers the ground, the vegetation indices indicated a mixture of plant and soil reflectance prior to the crop covering the soil. Future uses of remote sensing for agricultural issues will start to build relationships using machine learning and artificial intelligence to collect data with spatiotemporal properties. Artificial intelligence is already being applied to cropland suitability determination, and it has the potential to enhance both the interface between remotely gathered data and other data sources, as well as the updating of that data [3,77]. Assessing variations in crop emergence over time, crop vigor, and crop response to climatic conditions may be conducted using this kind of technique.

5. Conclusions

With the further development of low-cost UAVs and open-source software intended for processing data collected by the UAV in GIS, more opportunities to apply these systems in agriculture are expected. The development of UAV application in cropland suitability assessment is complimentary to precision agriculture, which enables performing agricultural fieldwork within agrotechnical deadlines, high productivity, a reduced number of operations, and the lowest cost of labor.

This study proposed a micro-scale approach for the cropland suitability assessment of permanent crops based on a low-cost UAV, achieving spectral and topographic aspects of cropland suitability for the tangerine plantation. Additionally, the application of open-source GIS software for supervised classification using machine learning algorithms and globally accepted FAO standard are expected to further improve the availability of its application for permanent crop plantation management. The performed study showed currently high suitability levels in both study subsets, with 63.1% suitable area in subset A and 59.0% in subset B. Despite that, the efficiency of agricultural production can be improved by managing crop, soil, and topographic properties in the currently non-suitable class (N1), providing recommendations for farmers for further agronomic inspection. The use of a low-cost RGB sensor justified its use for the study aim, and the amount of collected data can be expanded by using multispectral, hyperspectral, and thermal sensors. This increases the amount of collected data and enables the calculation of an even greater number of vegetation indices. Using a larger number of sensors increases the price of the UAV system, therefore, when buying a UAV, the farmers should carefully choose

which sensors are needed on a particular farm, taking into account the amount of arable land and the capabilities of those UAVs for the desired aim.

Author Contributions: conceptualization, D.R.; methodology, D.R.; software, D.R.; validation, D.R., I.P. and M.J.; formal analysis, M.J.; investigation, D.R., A.Š., I.P., and I.M.; resources, A.Š.; data curation, D.R., I.P., and I.M.; writing—original draft preparation, D.R.; writing—review and editing, D.R.; visualization, D.R.; supervision, M.J.; project administration, A.Š. and M.J.; funding acquisition, A.Š. All authors have read and agreed to the published version of the manuscript.

Funding: This research was performed within the project UIP-2017-05-2694 financially supported by the Croatian Science Foundation.

Data Availability Statement: Not applicable.

Acknowledgments: Authors would like to thank the Croatian Science Foundation for supporting this research.

Conflicts of Interest: The authors declare no conflicts of interest.

Appendix A

Table A1. Mean values of input data rasters per FAO suitability class.

Input Data Groups	Input Data	Mean Values per FAO Suitability Class				
		S1	S2	S3	N1	N2
Spectral bands	B	72.267	75.612	78.451	75.953	90.690
	G	139.740	123.815	131.218	116.605	116.053
	R	120.629	106.702	114.524	100.348	105.024
Spectral indices	NGRDI	0.078	0.084	0.076	0.088	0.063
	GLI	0.187	0.161	0.161	0.151	0.098
	BI	130.617	115.747	123.306	108.985	110.878
Topographic indices	Total insolation	1858.409	1230.934	1555.098	874.781	452.934
	Flow accumulation	3.234	4.904	7.209	4.071	5.759
	Wind exposition	1.066	1.030	1.034	1.023	0.989

References

1. Aldababseh, A.; Temimi, M.; Maghelal, P.; Branch, O.; Wulfmeyer, V. Multi-Criteria Evaluation of Irrigated Agriculture Suitability to Achieve Food Security in an Arid Environment. *Sustainability* **2018**, *10*, 803. https://doi.org/10.3390/su10030803.
2. Kurowska, K.; Marks-Bielska, R.; Bielski, S.; Aleknavičius, A.; Kowalczyk, C. Geographic Information Systems and the Sustainable Development of Rural Areas. *Land* **2021**, *10*, 6. https://doi.org/10.3390/land10010006.
3. Radočaj, D.; Jurišić, M.; Gašparović, M.; Plaščak, I.; Antonić, O. Cropland Suitability Assessment Using Satellite-Based Biophysical Vegetation Properties and Machine Learning. *Agronomy* **2021**, *11*, 1620. https://doi.org/10.3390/agronomy11081620.
4. Sasaki, K.; Hotes, S.; Ichinose, T.; Doko, T.; Wolters, V. Hotspots of Agricultural Ecosystem Services and Farmland Biodiversity Overlap with Areas at Risk of Land Abandonment in Japan. *Land* **2021**, *10*, 1031. https://doi.org/10.3390/land10101031.
5. Kanjir, U.; Đurić, N.; Veljanovski, T. Sentinel-2 Based Temporal Detection of Agricultural Land Use Anomalies in Support of Common Agricultural Policy Monitoring. *ISPRS Int. J. Geo-Inf.* **2018**, *7*, 405. https://doi.org/10.3390/ijgi7100405.
6. Jurišić, M.; Plaščak, I.; Antonić, O.; Radočaj, D. Suitability Calculation for Red Spicy Pepper Cultivation (Capsicum Annum L.) Using Hybrid GIS-Based Multicriteria Analysis. *Agronomy* **2020**, *10*, 3. https://doi.org/10.3390/agronomy10010003.
7. Binte Mostafiz, R.; Noguchi, R.; Ahamed, T. Agricultural Land Suitability Assessment Using Satellite Remote Sensing-Derived Soil-Vegetation Indices. *Land* **2021**, *10*, 223. https://doi.org/10.3390/land10020223.
8. Radočaj, D.; Jurišić, M. GIS-Based Cropland Suitability Prediction Using Machine Learning: A Novel Approach to Sustainable Agricultural Production. *Agronomy* **2022**, *12*, 2210. https://doi.org/10.3390/agronomy12092210.
9. AbdelRahman, M.A.E.; Natarajan, A.; Hegde, R. Assessment of Land Suitability and Capability by Integrating Remote Sensing and GIS for Agriculture in Chamarajanagar District, Karnataka, India. *Egypt. J. Remote Sens. Space Sci.* **2016**, *19*, 125–141. https://doi.org/10.1016/j.ejrs.2016.02.001.
10. Abolina, E.; Luzadis, V.A. Abandoned Agricultural Land and Its Potential for Short Rotation Woody Crops in Latvia. *Land Use Policy* **2015**, *49*, 435–445. https://doi.org/10.1016/j.landusepol.2015.08.022.

11. Belward, A.S.; Skøien, J.O. Who Launched What, When and Why; Trends in Global Land-Cover Observation Capacity from Civilian Earth Observation Satellites. *ISPRS J. Photogramm. Remote Sens.* **2015**, *103*, 115–128. https://doi.org/10.1016/j.isprsjprs.2014.03.009.
12. Zheng, J.; Song, X.; Yang, G.; Du, X.; Mei, X.; Yang, X. Remote Sensing Monitoring of Rice and Wheat Canopy Nitrogen: A Review. *Remote Sens.* **2022**, *14*, 5712. https://doi.org/10.3390/rs14225712.
13. Radocaj, D.; Obhodas, J.; Jurisic, M.; Gasparovic, M. Global Open Data Remote Sensing Satellite Missions for Land Monitoring and Conservation: A Review. *Land* **2020**, *9*, 402. https://doi.org/10.3390/land9110402.
14. Huang, C.; Chen, Y.; Zhang, S.; Wu, J. Detecting, Extracting, and Monitoring Surface Water From Space Using Optical Sensors: A Review. *Rev. Geophys.* **2018**, *56*, 333–360. https://doi.org/10.1029/2018RG000598.
15. Pelletier, C.; Valero, S.; Inglada, J.; Champion, N.; Dedieu, G. Assessing the Robustness of Random Forests to Map Land Cover with High Resolution Satellite Image Time Series over Large Areas. *Remote Sens. Environ.* **2016**, *187*, 156–168. https://doi.org/10.1016/j.rse.2016.10.010.
16. Lopez, R.; Frohn, R. *Remote Sensing for Landscape Ecology: New Metric Indicators*; 2nd ed.; CRC Press: Boca Raton, FL, USA, 2017; ISBN 978-1-315-15271-4.
17. Yao, H.; Qin, R.; Chen, X. Unmanned Aerial Vehicle for Remote Sensing Applications—A Review. *Remote Sens.* **2019**, *11*, 1443. https://doi.org/10.3390/rs11121443.
18. Pádua, L.; Vanko, J.; Hruška, J.; Adão, T.; Sousa, J.J.; Peres, E.; Morais, R. UAS, Sensors, and Data Processing in Agroforestry: A Review towards Practical Applications. *Int. J. Remote Sens.* **2017**, *38*, 2349–2391. https://doi.org/10.1080/01431161.2017.1297548.
19. Ammoniaci, M.; Kartsiotis, S.-P.; Perria, R.; Storchi, P. State of the Art of Monitoring Technologies and Data Processing for Precision Viticulture. *Agriculture* **2021**, *11*, 201. https://doi.org/10.3390/agriculture11030201.
20. Shi, X.; Han, W.; Zhao, T.; Tang, J. Decision Support System for Variable Rate Irrigation Based on UAV Multispectral Remote Sensing. *Sensors* **2019**, *19*, 2880. https://doi.org/10.3390/s19132880.
21. Reddy Maddikunta, P.K.; Hakak, S.; Alazab, M.; Bhattacharya, S.; Gadekallu, T.R.; Khan, W.Z.; Pham, Q.-V. Unmanned Aerial Vehicles in Smart Agriculture: Applications, Requirements, and Challenges. *IEEE Sens. J.* **2021**, *21*, 17608–17619. https://doi.org/10.1109/JSEN.2021.3049471.
22. Chen, S.; Lan, Y.; Zhou, Z.; Ouyang, F.; Wang, G.; Huang, X.; Deng, X.; Cheng, S. Effect of Droplet Size Parameters on Droplet Deposition and Drift of Aerial Spraying by Using Plant Protection UAV. *Agronomy* **2020**, *10*, 195. https://doi.org/10.3390/agronomy10020195.
23. Candiago, S.; Remondino, F.; De Giglio, M.; Dubbini, M.; Gattelli, M. Evaluating Multispectral Images and Vegetation Indices for Precision Farming Applications from UAV Images. *Remote Sens.* **2015**, *7*, 4026–4047. https://doi.org/10.3390/rs70404026.
24. Barrero, O.; Perdomo, S.A. RGB and Multispectral UAV Image Fusion for Gramineae Weed Detection in Rice Fields. *Precis. Agric.* **2018**, *19*, 809–822. https://doi.org/10.1007/s11119-017-9558-x.
25. Blancon, J.; Dutartre, D.; Tixier, M.-H.; Weiss, M.; Comar, A.; Praud, S.; Baret, F. A High-Throughput Model-Assisted Method for Phenotyping Maize Green Leaf Area Index Dynamics Using Unmanned Aerial Vehicle Imagery. *Front. Plant Sci.* **2019**, *10*, 685.
26. Maimaitijiang, M.; Sagan, V.; Sidike, P.; Maimaitiyiming, M.; Hartling, S.; Peterson, K.T.; Maw, M.J.W.; Shakoor, N.; Mockler, T.; Fritschi, F.B. Vegetation Index Weighted Canopy Volume Model (CVMVI) for Soybean Biomass Estimation from Unmanned Aerial System-Based RGB Imagery. *ISPRS J. Photogramm. Remote Sens.* **2019**, *151*, 27–41. https://doi.org/10.1016/j.isprsjprs.2019.03.003.
27. Schirrmann, M.; Giebel, A.; Gleiniger, F.; Pflanz, M.; Lentschke, J.; Dammer, K.-H. Monitoring Agronomic Parameters of Winter Wheat Crops with Low-Cost UAV Imagery. *Remote Sens.* **2016**, *8*, 706. https://doi.org/10.3390/rs8090706.
28. Gašparović, M.; Zrinjski, M.; Barković, Đ.; Radočaj, D. An Automatic Method for Weed Mapping in Oat Fields Based on UAV Imagery. *Comput. Electron. Agric.* **2020**, *173*, 105385. https://doi.org/10.1016/j.compag.2020.105385.
29. Cano, M. de J.A.; Marulanda, E.E.C.; Henao-Céspedes, V.; Cardona-Morales, O.; Garcés-Gómez, Y.A. Quantification of Flowering in Coffee Growing with Low-Cost RGB Sensor UAV-Mounted. *Sci. Hortic.* **2023**, *309*, 111649. https://doi.org/10.1016/j.scienta.2022.111649.
30. Akpoti, K.; Kabo-bah, A.T.; Dossou-Yovo, E.R.; Groen, T.A.; Zwart, S.J. Mapping Suitability for Rice Production in Inland Valley Landscapes in Benin and Togo Using Environmental Niche Modeling. *Sci. Total Environ.* **2020**, *709*, 136165. https://doi.org/10.1016/j.scitotenv.2019.136165.
31. Iliquín Trigoso, D.; Salas López, R.; Rojas Briceño, N.B.; Silva López, J.O.; Gómez Fernández, D.; Oliva, M.; Quiñones Huatangari, L.; Terrones Murga, R.E.; Barboza Castillo, E.; Barrena Gurbillón, M.Á. Land Suitability Analysis for Potato Crop in the Jucusbamba and Tincas Microwatersheds (Amazonas, NW Peru): AHP and RS–GIS Approach. *Agronomy* **2020**, *10*, 1898. https://doi.org/10.3390/agronomy10121898.
32. Fareed, N.; Rehman, K. Integration of Remote Sensing and GIS to Extract Plantation Rows from A Drone-Based Image Point Cloud Digital Surface Model. *ISPRS Int. J. Geo-Inf.* **2020**, *9*, 151. https://doi.org/10.3390/ijgi9030151.
33. Croatian Meteorological and Hydrological Service, Climate Atlas of Croatia 1961–1990, 1971–2000. Available online: https://klima.hr/razno/publikacije/klimatski_atlas_hrvatske.pdf (accessed on 18 January 2023).
34. Republic of Croatia, State Geodetic Administration CROPOS Users' Manual 2011. Available online: https://www.cropos.hr/files/docs/cropos_users-manual.pdf (accessed on 22 November 2021).

35. Vellemu, E.C.; Katonda, V.; Yapuwa, H.; Msuku, G.; Nkhoma, S.; Makwakwa, C.; Safuya, K.; Maluwa, A. Using the Mavic 2 Pro Drone for Basic Water Quality Assessment. *Sci. Afr.* **2021**, *14*, e00979. https://doi.org/10.1016/j.sciaf.2021.e00979.
36. Jiang, J.; Cai, W.; Zheng, H.; Cheng, T.; Tian, Y.; Zhu, Y.; Ehsani, R.; Hu, Y.; Niu, Q.; Gui, L.; et al. Using Digital Cameras on an Unmanned Aerial Vehicle to Derive Optimum Color Vegetation Indices for Leaf Nitrogen Concentration Monitoring in Winter Wheat. *Remote Sens.* **2019**, *11*, 2667. https://doi.org/10.3390/rs11222667.
37. Mao, P.; Qin, L.; Hao, M.; Zhao, W.; Luo, J.; Qiu, X.; Xu, L.; Xiong, Y.; Ran, Y.; Yan, C.; et al. An Improved Approach to Estimate Above-Ground Volume and Biomass of Desert Shrub Communities Based on UAV RGB Images. *Ecol. Indic.* **2021**, *125*, 107494. https://doi.org/10.1016/j.ecolind.2021.107494.
38. Abrougui, K.; Boughattas, N.E.H.; Belhaj, M.; Buchaillot, M.L.; Segarra, J.; Dorbolo, S.; Amami, R.; Chehaibi, S.; Tarchoun, N.; Kefauver, S.C. Assessing Phytosanitary Application Efficiency of a Boom Sprayer Machine Using RGB Sensor in Grassy Fields. *Sustainability* **2022**, *14*, 3666. https://doi.org/10.3390/su14063666.
39. Liu, X.; Wang, L. Feasibility of Using Consumer-Grade Unmanned Aerial Vehicles to Estimate Leaf Area Index in Mangrove Forest. *Remote Sens. Lett.* **2018**, *9*, 1040–1049. https://doi.org/10.1080/2150704X.2018.1504339.
40. Tucker, C.J. Red and Photographic Infrared Linear Combinations for Monitoring Vegetation. *Remote Sens. Environ.* **1979**, *8*, 127–150. https://doi.org/10.1016/0034-4257(79)90013-0.
41. Louhaichi, M.; Borman, M.M.; Johnson, D.E. Spatially Located Platform and Aerial Photography for Documentation of Grazing Impacts on Wheat. *Geocarto Int.* **2001**, *16*, 65–70. https://doi.org/10.1080/10106040108542184.
42. Kawashima, S.; Nakatani, M. An Algorithm for Estimating Chlorophyll Content in Leaves Using a Video Camera. *Ann. Bot.* **1998**, *81*, 49–54. https://doi.org/10.1006/anbo.1997.0544.
43. Böhner, J.; Antonić, O. Chapter 8 Land-Surface Parameters Specific to Topo-Climatology. In *Developments in Soil Science*; Hengl, T., Reuter, H.I., Eds.; Geomorphometry; Elsevier: Amsterdam, The Netherlands, 2009; Volume 33; pp. 195–226.
44. Conrad, O.; Bechtel, B.; Bock, M.; Dietrich, H.; Fischer, E.; Gerlitz, L.; Wehberg, J.; Wichmann, V.; Boehner, J. System for Automated Geoscientific Analyses (SAGA) v. 2.1.4. *Geosci. Model Dev.* **2015**, *8*, 1991–2007. https://doi.org/10.5194/gmd-8-1991-2015.
45. Freeman, T.G. Calculating Catchment Area with Divergent Flow Based on a Regular Grid. *Comput. Geosci.* **1991**, *17*, 413–422. https://doi.org/10.1016/0098-3004(91)90048-I.
46. Bagaram, M.B.; Giuliarelli, D.; Chirici, G.; Giannetti, F.; Barbati, A. UAV Remote Sensing for Biodiversity Monitoring: Are Forest Canopy Gaps Good Covariates? *Remote Sens.* **2018**, *10*, 1397. https://doi.org/10.3390/rs10091397.
47. FAO Chapter 3: Land Suitability Classifications 1976. Available online: https://www.fao.org/3/x5310e/x5310e04.htm#chapter%203:%20land%20suitability%20classifications (accessed on 13 July 2022).
48. Radočaj, D.; Jurišić, M.; Gašparović, M. The Role of Remote Sensing Data and Methods in a Modern Approach to Fertilization in Precision Agriculture. *Remote Sens.* **2022**, *14*, 778. https://doi.org/10.3390/rs14030778.
49. Rodriguez-Galiano, V.F.; Chica-Rivas, M. Evaluation of Different Machine Learning Methods for Land Cover Mapping of a Mediterranean Area Using Multi-Seasonal Landsat Images and Digital Terrain Models. *Int. J. Digit. Earth* **2014**, *7*, 492–509. https://doi.org/10.1080/17538947.2012.748848.
50. Congalton, R.G.; Green, K. *Assessing the Accuracy of Remotely Sensed Data: Principles and Practices*; 3rd ed.; CRC Press: Boca Raton, FL, USA, 2019; ISBN 978-0-429-05272-9.
51. FAO Chapter 1: The Nature and Principles of Land Evaluation 1976. Available online: https://www.fao.org/3/x5310e/x5310e02.htm#chapter%201:%20the%20nature%20and%20principles%20of%20land%20evaluation (accessed on 13 July 2022).
52. Said Mohamed, E.; Belal, AA.; Kotb Abd-Elmabod, S.; El-Shirbeny, M.A.; Gad, A.; Zahran, M.B. Smart Farming for Improving Agricultural Management. *Egypt. J. Remote Sens. Space Sci.* **2021**, *24*, 971–981. https://doi.org/10.1016/j.ejrs.2021.08.007.
53. Awais, M.; Li, W.; Cheema, M.J.M.; Zaman, Q.U.; Shaheen, A.; Aslam, B.; Zhu, W.; Ajmal, M.; Faheem, M.; Hussain, S.; et al. UAV-Based Remote Sensing in Plant Stress Imagine Using High-Resolution Thermal Sensor for Digital Agriculture Practices: A Meta-Review. *Int. J. Environ. Sci. Technol.* **2022**, *20*, 1135–1152. https://doi.org/10.1007/s13762-021-03801-5.
54. Giovos, R.; Tassopoulos, D.; Kalivas, D.; Lougkos, N.; Priovolou, A. Remote Sensing Vegetation Indices in Viticulture: A Critical Review. *Agriculture* **2021**, *11*, 457. https://doi.org/10.3390/agriculture11050457.
55. Goddijn-Murphy, L.; O'Hanlon, N.J.; James, N.A.; Masden, E.A.; Bond, A.L. Earth Observation Data for Seabirds and Their Habitats: An Introduction. *Remote Sens. Appl. Soc. Environ.* **2021**, *24*, 100619. https://doi.org/10.1016/j.rsase.2021.100619.
56. Ji, S.; Gu, C.; Xi, X.; Zhang, Z.; Hong, Q.; Huo, Z.; Zhao, H.; Zhang, R.; Li, B.; Tan, C. Quantitative Monitoring of Leaf Area Index in Rice Based on Hyperspectral Feature Bands and Ridge Regression Algorithm. *Remote Sens.* **2022**, *14*, 2777. https://doi.org/10.3390/rs14122777.
57. Banerjee, A.; Roychoudhury, A. *Role of Phenomics in Screening Abiotic Stress Tolerance in Plants*; Apple Academic Press: Palm Bay, FL, USA, 2022; pp. 47–59; ISBN 978-1-00-318057-9.
58. Hunt, E.R.; Cavigelli, M.; Daughtry, C.S.T.; Mcmurtrey, J.E.; Walthall, C.L. Evaluation of Digital Photography from Model Aircraft for Remote Sensing of Crop Biomass and Nitrogen Status. *Precis. Agric.* **2005**, *6*, 359–378. https://doi.org/10.1007/s11119-005-2324-5.
59. E. D. Chaves, M.; C. A. Picoli, M.; D. Sanches, I. Recent Applications of Landsat 8/OLI and Sentinel-2/MSI for Land Use and Land Cover Mapping: A Systematic Review. *Remote Sens.* **2020**, *12*, 3062. https://doi.org/10.3390/rs12183062.
60. García-Martínez, H.; Flores-Magdaleno, H.; Ascencio-Hernández, R.; Khalil-Gardezi, A.; Tijerina-Chávez, L.; Mancilla-Villa, O.R.; Vázquez-Peña, M.A. Corn Grain Yield Estimation from Vegetation Indices, Canopy Cover, Plant Density, and a Neural

Network Using Multispectral and RGB Images Acquired with Unmanned Aerial Vehicles. *Agriculture* **2020**, *10*, 277. https://doi.org/10.3390/agriculture10070277.
61. Hunt, E.R.; Doraiswamy, P.C.; McMurtrey, J.E.; Daughtry, C.S.T.; Perry, E.M.; Akhmedov, B. A Visible Band Index for Remote Sensing Leaf Chlorophyll Content at the Canopy Scale. *Int. J. Appl. Earth Obs. Geoinf.* **2013**, *21*, 103–112. https://doi.org/10.1016/j.jag.2012.07.020.
62. Mitchell, S.; Weersink, A.; Erickson, B. Adoption of Precision Agriculture Technologies in Ontario Crop Production. *Can. J. Plant Sci.* **2018**, *98*, 1384–1388. https://doi.org/10.1139/cjps-2017-0342.
63. Jurišić, M.; Radočaj, D.; Plaščak, I.; Galić Subašić, D.; Petrović, D. The evaluation of the RGB and multispectral camera on the unmanned aerial vehicle (UAV) for the machine learning classification of Maize. *Poljoprivreda* **2022**, *28*, 74–80. https://doi.org/10.18047/poljo.28.2.10.
64. Ye, H.; Huang, W.; Huang, S.; Cui, B.; Dong, Y.; Guo, A.; Ren, Y.; Jin, Y. Identification of Banana Fusarium Wilt Using Supervised Classification Algorithms with UAV-Based Multi-Spectral Imagery. *Int. J. Agric. Biol. Eng.* **2020**, *13*, 136–142. https://doi.org/10.25165/j.ijabe.20201303.5524.
65. Zha, H.; Miao, Y.; Wang, T.; Li, Y.; Zhang, J.; Sun, W.; Feng, Z.; Kusnierek, K. Improving Unmanned Aerial Vehicle Remote Sensing-Based Rice Nitrogen Nutrition Index Prediction with Machine Learning. *Remote Sens.* **2020**, *12*, 215. https://doi.org/10.3390/rs12020215.
66. Syazwani, R.W.N.; Asraf, M.H.; Amin, M.A.M.S.; Dalil, K.A.N. Automated Image Identification, Detection and Fruit Counting of Top-View Pineapple Crown Using Machine Learning. *Alex. Eng. J.* **2022**, *61*, 1265–1276. https://doi.org/10.1016/j.aej.2021.06.053.
67. Khan, N.; Kamaruddin, M.A.; Sheikh, U.U.; Yusup, Y.; Bakht, M.P. Oil Palm and Machine Learning: Reviewing One Decade of Ideas, Innovations, Applications, and Gaps. *Agriculture* **2021**, *11*, 832. https://doi.org/10.3390/agriculture11090832.
68. Padua, L.; Adao, T.; Hruska, J.; Guimaraes, N.; Marques, P.; Peres, E.; Sousa, J.J. Vineyard Classification Using Machine Learning Techniques Applied to Rgb-Uav Imagery. In *Proceedings of the IGARSS 2020 IEEE International Geoscience and Remote Sensing Symposium, Waikoloa, HI, USA, 26 September–2 October 2020;* IEEE: New York, NY, USA, 2020; pp. 6309–6312.
69. Republic of Croatia, Ministry of Agriculture. Regulations on Methodology for Monitoring the Condition of Agricultural Land. Available online: https://narodne-novine.nn.hr/clanci/sluzbeni/full/2019_05_47_918.html (accessed on 19 January 2023).
70. Gluhić, D. Supply level of nutrients in tangerine growing soils in the Neretva valley. *Glas. Zašt. Bilja* **2006**, *29*, 39–47.
71. Milošević, T.; Milošević, N.; Mladenović, J. The Influence of Organic, Organo-Mineral and Mineral Fertilizers on Tree Growth, Yielding, Fruit Quality and Leaf Nutrient Composition of Apple Cv. 'Golden Delicious Reinders. *Sci. Hortic.* **2022**, *297*, 110978. https://doi.org/10.1016/j.scienta.2022.110978.
72. Green, S.; Cawkwell, F.; Dwyer, E. A Time-Domain NDVI Anomaly Service for Intensively Managed Grassland Agriculture. *Remote Sens. Appl. Soc. Environ.* **2018**, *11*, 282–290. https://doi.org/10.1016/j.rsase.2018.07.011.
73. Radočaj, D.; Jurišić, M.; Gašparović, M.; Plaščak, I. Optimal Soybean (Glycine Max L.) Land Suitability Using GIS-Based Multicriteria Analysis and Sentinel-2 Multitemporal Images. *Remote Sens.* **2020**, *12*, 1463. https://doi.org/10.3390/rs12091463.
74. Claverie, M.; Demarez, V.; Duchemin, B.; Hagolle, O.; Ducrot, D.; Marais-Sicre, C.; Dejoux, J.-F.; Huc, M.; Keravec, P.; Béziat, P.; et al. Maize and Sunflower Biomass Estimation in Southwest France Using High Spatial and Temporal Resolution Remote Sensing Data. *Remote Sens. Environ.* **2012**, *124*, 844–857. https://doi.org/10.1016/j.rse.2012.04.005.
75. Guan, K.; Wu, J.; Kimball, J.S.; Anderson, M.C.; Frolking, S.; Li, B.; Hain, C.R.; Lobell, D.B. The Shared and Unique Values of Optical, Fluorescence, Thermal and Microwave Satellite Data for Estimating Large-Scale Crop Yields. *Remote Sens. Environ.* **2017**, *199*, 333–349. https://doi.org/10.1016/j.rse.2017.06.043.
76. Zarco-Tejada, P.J.; González-Dugo, M.V.; Fereres, E. Seasonal Stability of Chlorophyll Fluorescence Quantified from Airborne Hyperspectral Imagery as an Indicator of Net Photosynthesis in the Context of Precision Agriculture. *Remote Sens. Environ.* **2016**, *179*, 89–103. https://doi.org/10.1016/j.rse.2016.03.024.
77. Wang, M.; Wander, M.; Mueller, S.; Martin, N.; Dunn, J.B. Evaluation of Survey and Remote Sensing Data Products Used to Estimate Land Use Change in the United States: Evolving Issues and Emerging Opportunities. *Environ. Sci. Policy* **2022**, *129*, 68–78. https://doi.org/10.1016/j.envsci.2021.12.021.